The CKM Matrix in the Era of the B Factories

Andreas Höcker
Laboratoire de l'Accélérateur Linéaire
IN2P3-CNRS et Université de Paris-Sud
BP 34
F-91898 Orsay Cedex, France

1 Introduction

Until the establishment of *CP* violation (CPV) in the B sector by *BABAR* [1] and Belle [2] in Summer 2001, global CKM analyses [9] primarily attempted to predict yet unmeasured observables like, *e.g.*, the three angles of the unitary triangle of the B sector. Indeed, as pointed out by Bigi [3]: "in '98 courageous souls predicted $\sin 2\beta \sim 0.73 \pm 0.06$ [4]", which turned out to be in excellent agreement with the direct measurement (the present world average reads $\sin 2\beta = 0.78 \pm 0.08$ [5]). Since then more and more measurements of *CP* asymmetries and rare decays emerge from the breathlessly operating B factories. They qualify us to significantly probe the Standard Model (SM) and to search for contributions from new physics. Obviously, predictions are still valuable in the sectors of rare K and B decays in order to assess the necessary sensitivities experiments have to provide in order to perform meaningful measurements. Both goals require a robust and sufficiently conservative approach to accommodate a global fit of observables the theoretical predictions of which are often dominated by hardly accountable systematic uncertainties of theoretical origin.

2 *CP* Violation in the Standard Model

In the Standard Model of three quark generations, CPV is generated by a single phase in the unitary CKM matrix [8], governing flavor changing charged currents. Throughout this review, the Wolfenstein parameterization [10] of the CKM matrix is used. It expands the matrix elements in terms of powers of $\lambda = V_{us} \sim 0.2$ so that one finds for the diagonal elements $|V_{ud}| \sim |V_{cs}| \sim |V_{tb}| \sim 1$, and for the off-diagonal elements $|V_{us}| \sim |V_{cd}| \sim \lambda$, $|V_{cb}| \sim |V_{ts}| \sim \lambda^2$, $|V_{ub}| \sim |V_{td}| \sim \lambda^3$. The CKM phase is given by $\tan^{-1}(\overline{\eta}/\overline{\rho})$, with $\overline{\rho}(\overline{\eta}) = \rho(\eta)(1 - \lambda^2/2)$ [11] so that one can elegantly display the available constraints in the complex $\overline{\rho} - \overline{\eta}$ plane, representing the (rescaled) *Unitarity Triangle* (UT):

$$\frac{V_{ud}V_{ub}^*}{V_{cd}V_{cb}^*} + 1 + \frac{V_{td}V_{tb}^*}{V_{cd}V_{cb}^*} = 0 \; . \tag{1}$$

It is interesting to note that multiplying the $\overline{\rho} - \overline{\eta}$ plane by a phase, rotates the UT while leaving its surface invariant. Hence, the surface of the UT represents a phase-convention invariant quantity which measures CPV. A more general form of this has been given by C. Jarlskog [12]:

$$\mathrm{Im}\left[V_{ij}V_{kl}V_{il}^{*}V_{kj}^{*}\right] = J\sum_{m,n=1}^{3}\epsilon_{ikm}\epsilon_{jln}\ , \tag{2}$$

(with ϵ_{ikm} being the total antisymmetric tensor) corresponding to twice the (*non-rescaled*) UT (1). The empirical value of J is small compared to its geometrical maximum of $1/(6\sqrt{3}) \simeq 0.1$, showing that CP violation is suppressed as a consequence of the strong hierarchy exhibited by the CKM matrix elements. It is the remarkable outcome of the derivation of J, involving the commutator of the up-type and down-type unitary mass matrices, that CPV requires not only J to be non-zero, but also the existence of a non-degenerated mass hierarchy. Equal masses between at least two generations of up-type or down-type quarks would remove the CKM phase.

Over-determining the CKM phase with the ambition to discover new physics represents the primary motivation to study B decays in the era of the B factories. Direct or indirect constraints on the CKM phase are collected from the following sources:

- CPV in the B and the K systems. Studied are three types: (i), CPV in interference of decays with and without mixing, (ii), CPV in mixing and (iii), CPV in the interference between decay amplitudes (often called *direct* CPV).

- $B_d^0\overline{B}_d^0$ and $B_s^0\overline{B}_s^0$ mixing.

- direct determination of the matrix element $|V_{ub}|$ (and $|V_{cb}|$) by means of exclusive and inclusive rate measurements.

- detection of rare K and B decays.

A graphical compilation of the most relevant present and future constraints, sensitive to the *CP*-violating phase, is displayed in Fig. 1. The UT (1) is indicated by the hatched area. Its three angles α, β and γ (or, in the trigonometric order: $\phi_1 \equiv \beta$, $\phi_2 \equiv \alpha$, $\phi_3 \equiv \gamma$) and two non-trivial sides are determined by the processes described above. More precisely, the sides and the angle γ are measured by tree level processes, while α and β are determined from loop induced processes. Only the latter are believed to be sensitive to new physics so that the comparison with the former effectively probes the SM.

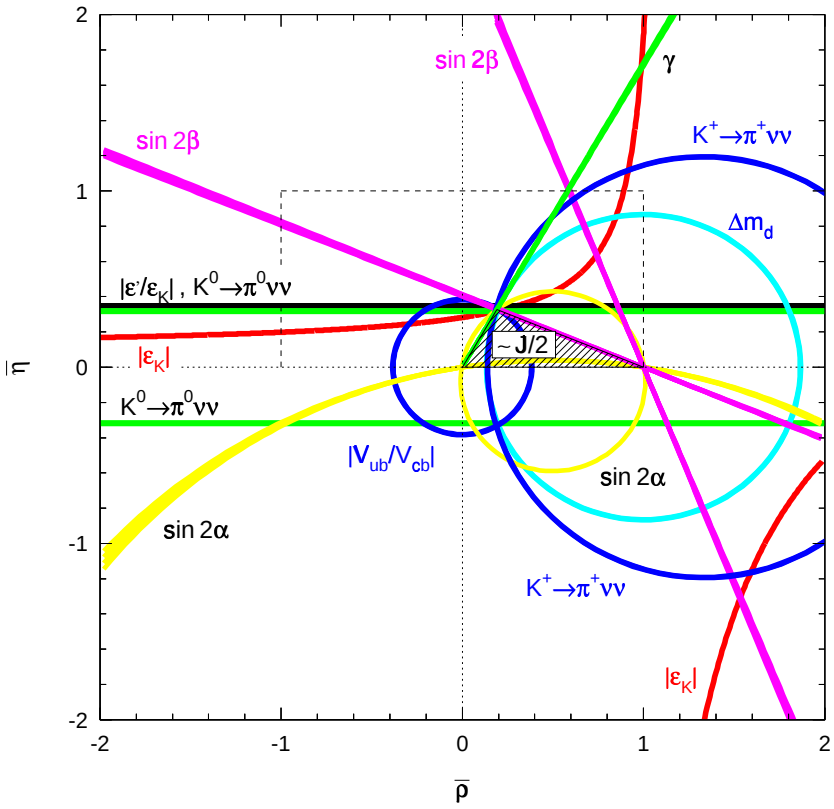

Figure 1: What is the value of J in our world? Constraints in the $\overline{\rho} - \overline{\eta}$ plane for the most relevant observables. The theoretical parameters used correspond to some "standard" set chosen to reproduce compatibility. The unitarity triangle on which we concentrate in the following for the global fit is indicated by the hatched area. It's surface is proportional to the Jarlskog parameter J (*c.f.*, Eq. (2)).

3 The Standard CKM Analysis

Table 1 represents an attempt to categorize the abundance of the constraints that can be (or will in the near future be) used in a global CKM determination[1]. The "star" system qualifies mainly the concern of theoretical uncertainties in the SM prediction of a given observable. At present, the only measurements to which three stars shall be attributed are the determination of λ from rates of $u \to d$ and $u \to s$

[1]The most promising measurements on B_s decays that will be performed at the hadron colliders TEVATRON and LHC are not yet taken into account.

Observables	CKM Parameters	Experimental Sources	Theoretical Uncertainties	Quality
$\lvert V_{ud}\rvert$	λ	nuclear β decay	small	$\star\star\star$
$\lvert V_{us}\rvert$		$K \to \pi e \nu_e$		
ϵ_K	$\overline{\eta} \propto (1-\overline{\rho})^{-1}$	$K^0 \to \pi^+\pi^-,\ \pi^0\pi^0$	B_K, η_{cc}	$\star$
ϵ'/ϵ_K	$\overline{\eta}$	$K^0 \to \pi^+\pi^-,\ \pi^0\pi^0$	B_6, B_8	?
$\mathrm{Im}^2[V_{ts}^* V_{td} \ldots]$	$(\lambda^2 A)^4 \overline{\eta}^2$	$K_L^0 \to \pi^0 \nu\overline{\nu}$	small [but: $\propto (\lambda^2 A)^4$]	$\star\star\,(\star)$
$\lvert V_{td}\rvert$	$(1-\overline{\rho})^2 + \overline{\eta}^2$	$K^+ \to \pi^+ \nu\overline{\nu}$	charm loop, [$\propto (\lambda^2 A)^4$]	$\star\,(\star)$
Δm_d ($\lvert V_{td}\rvert$)	$(1-\overline{\rho})^2 + \overline{\eta}^2$	$B_d^0 \overline{B}_d^0$ mixing	$f_{B_d}\sqrt{B_d}$	$\star$
Δm_s ($\lvert V_{ts}\rvert$, ξ)	A	$B_s^0 \overline{B}_s^0$ mixing	$\xi = f_{B_s}\sqrt{B_s}/f_{B_d}\sqrt{B_d}$	$\star\star$
$\sin 2\beta$	$\overline{\rho}$, $\overline{\eta}$	$(\overline{b}d) \to (\overline{c}c,\ \overline{s}s)(\overline{s}d)$	small	$\star\star\star$
$\sin 2\alpha$	$\overline{\rho}$, $\overline{\eta}$	$(\overline{b}d) \to (u\overline{d})(\overline{u}d)$	penguins	?
γ	$\overline{\rho}$, $\overline{\eta}$	$B \to DK$	small (statistics?)	$\star\star$
		$b \to u$, direct CPV	penguins	?
$\lvert V_{cb}\rvert$	A	$b \to c\ell\nu$ (excl./incl.)	$F_{D^*}(1)$/OPE	$\star\star$
$\lvert V_{ub}\rvert$	$\overline{\rho}^2 + \overline{\eta}^2$	$b \to u\ell\nu$ (excl./incl.)	model/OPE	$\star\star$
$\lvert V_{td}\rvert$	$(1-\overline{\rho})^2 + \overline{\eta}^2$	$B_d \to \rho\gamma$	model	?
$\lvert V_{ts}\rvert$	A (new phys.)	$B_d \to X_s(\mathrm{or}: K^{(*)})\gamma$	model	?
		$B_d \to K^{(*)}\ell^+\ell^-$ (FCNC)		
$\lvert V_{ub}\rvert$ (f_{B_d})	$\overline{\rho}^2 + \overline{\eta}^2$	$B^+ \to \tau^+ \nu_\tau$	f_{B_d}	$\star\star$

Table 1: Observables sensitive to the CKM matrix elements.

transitions[2], and the prominent $\sin 2\beta$ measured in of a time-dependent analysis using $(\overline{b}d) \to (\overline{c}c,\ \overline{s}s)(\overline{s}d)$ CP eigenstates. The charmonium modes being tree dominated and the $\overline{s}s$ modes being penguin dominated (for which larger scales are involved), the independent measurements of both modes represent a powerful probe of new physics. A number of observables suffer from significant theoretical uncertainties mainly due to long distance QCD of non-perturbative origin. Some of them will be discussed below.

3.1 Fit technique

This review heavily employs the framework package *CKMfitter* [6], featuring the statistical approach *R*fit [7], which is based on a frequentist understanding of systematic theoretical uncertainties. No probability distributions are assumed for theoretical

[2]The apparent up to 3σ incompatibility between the determination of λ from $\lvert V_{ud}\rvert$ and $\lvert V_{us}\rvert$, respectively, is not limiting the determination of the CKM phase, as far as one can assume that only large scale phenomena are responsible for physics beyond the SM (see also Ref. [14]).

parameters. The CKM analysis is performed in three stages:

1. *Probing the SM*: the overall consistency between data and the theoretical framework, here the SM, is tested by means of a Monte Carlo simulation.

2. *Metrology*: if the agreement between data and the SM is found to be acceptable, confidence levels (CL) in parameter subspaces are determined.

3. *Probing new physics*: extensions of the SM are tested and limits on new physics parameters are determined.

Since the CL obtained for the SM in the first step of the CKM analysis is found to be sufficient (57%), we will concentrate on the metrology phase (step 2) in this review. Due to the lack of space, tests of new physics are not discussed. The reader is referred to Ref. [13] for an example application to $B^0_d\overline{B}^0_d$ mixing using *R*fit. If the hypothesis "the CKM picture of the SM is correct" is accepted, CLs in parameter subspaces (*e.g.*, $\overline{\rho}-\overline{\eta}$) are evaluated by means of fine granular scans. For a given point in a subspace, one determines the best agreement between data and theory. One obtains the quantity $\Delta\chi^2$ by varying freely all model parameters with the exception of those that are scanned in the subspace. After fitting, the corresponding CL is obtained from $\mathrm{CL} = \mathrm{Prob}(\Delta\chi^2, N_{\mathrm{dof}})$, where N_{dof} is the number of degrees of freedom, which in general coincides with the dimension of the subspace.

3.2 Fit inputs

The input observables and parameters used for the standard CKM fit are listed in Table 2.

A precise knowledge of $|V_{ub}|$ is required for a comparison with the loop-induced $\sin 2\beta$ (search for new physics). The element $|V_{cb}|$ is an important ingredient of the SM predictions of observables from kaon physics, in particular the rates of rare kaon decays. Theoretical uncertainties are sizeable for the determination of $|V_{ub}|$ and $|V_{cb}|$ from exclusive and inclusive semileptonic $b \to u$ and $b \to c$ transitions, respectively. The theoretical analyses intensively employ *Heavy Quark Symmetry*[3]. The computation tools are *Heavy Quark Effective Theory* and the *Operator Product Expansion* (OPE), where the latter organizes short and long-distance contributions in a power series of $\lambda_{\mathrm{QCD}}/m_b$ and $\alpha_s(m_b)$. On the exclusive side, the knowledge of the corresponding weak transition form factor is crucial, the prediction of which is model-dependent [23]. In principle, fully inclusive decays do not suffer from this drawback. This is however no longer true once experimental cuts are involved [24]. In particular, $b \to u$ transitions

[3] In the $m_Q \to \infty$ limit, the heavy quark represents a static color source with fixed four-momentum so that the light degrees of freedom become insensitive to spin and flavor of the heavy quark.

Observable/Parameter	Value ± error	Source
$\|V_{ub}\|$	$(3.25\,^{+0.25}_{-0.32} \pm 0.55) \times 10^{-3}$	CLEO exclusive [17]
$\|V_{ub}\|$	$(4.08 \pm 0.56 \pm 0.40) \times 10^{-3}$	CLEO inclusive & moments [15]
$\|V_{ub}\|$	$(4.09 \pm 0.61 \pm 0.42) \times 10^{-3}$	LEP inclusive [16]
$F_{D^\star}(1)\|V_{cb}\|$	$(35.4 \pm 1.9 \pm 1.8) \times 10^{-3}$	Belle exclusive [18]
$F_{D^\star}(1)\|V_{cb}\|$	$(43.1 \pm 1.3 \pm 1.8) \times 10^{-3}$	CLEO exclusive [19]
$F_{D^\star}(1)\|V_{cb}\|$	$(38.2 \pm 1.1) \times 10^{-3}$	LEP exclusive [21]
$\|V_{cb}\|$	$(40.4 \pm 1.0 \pm 0.8) \times 10^{-3}$	CLEO inclusive & moments [20]
Δm_d	(0.496 ± 0.007) ps^{-1}	WA
Δm_s	Amplitude Spectrum	WA [22]
$\sin 2\beta$	0.78 ± 0.08	WA [5]
$m_t(\overline{\rm MS})$	(166 ± 5) GeV/c^2	PDG'00
$f_{B_d}\sqrt{B_d}$	$(230 \pm 28 \pm 28)$ MeV	Lattice 2000
ξ	$(1.16 \pm 0.03 \pm 0.05)$ MeV	Lattice 2000
B_K	$(0.87 \pm 0.06 \pm 0.13)$ MeV	Lattice 2000

Table 2: Values and errors of some of the most relevant CKM fit input observables and parameters. Averages of uncorrelated determinations of the same observables are obtained in a natural way using the product of the corresponding likelihoods. For $|V_{ub}|$ and $|V_{cb}|$, the first errors are experimental and the second theoretical. For $F_{D^\star}(1)|V_{cb}|$, the first errors are statistical and the second systematic. The relevant $B \to D^*\ell\nu$ form factor is $F_{D^\star}(1) \simeq 0.91 \pm 0.04$ (see refs. and discussion in [7]). We use the averaged amplitude spectrum to incorporate the $B^0_s\overline{B}^0_s$ oscillation results [22]. The standard CKM analysis is theoretically limited (with the exception of $\sin 2\beta$).

are largely overcast by $b \to c$ background events. Kinematic cuts allow to reduce this background to the cost of a loss of inclusiveness and thus a rise of the theoretical uncertainty. A precise measurement of the *shape function* representing the Fermi motion of the b quark within the B meson (the light quark (*light degrees of freedom*) "knocks" at the heavy quark) could significantly reduce the theoretical uncertainties on the cuts applied. A useful shape function can be extracted from $B \to s\gamma$ decays, using some theoretical input for higher order corrections of the transfer function [15, 24].

The combined use of Δm_d and Δm_s improves the theoretically limited prediction of the individual $B^0\overline{B}^0$ mixing frequencies by a factor of about 3.6, since only the relative frequencies are involved (see Ref. [25] for recent criticism concerning the precision of ξ). The experimental information on $B^0_s\overline{B}^0_s$ mixing is yet insufficient to claim a signal. We use the averaged amplitude spectrum [22] and compute from it the expected

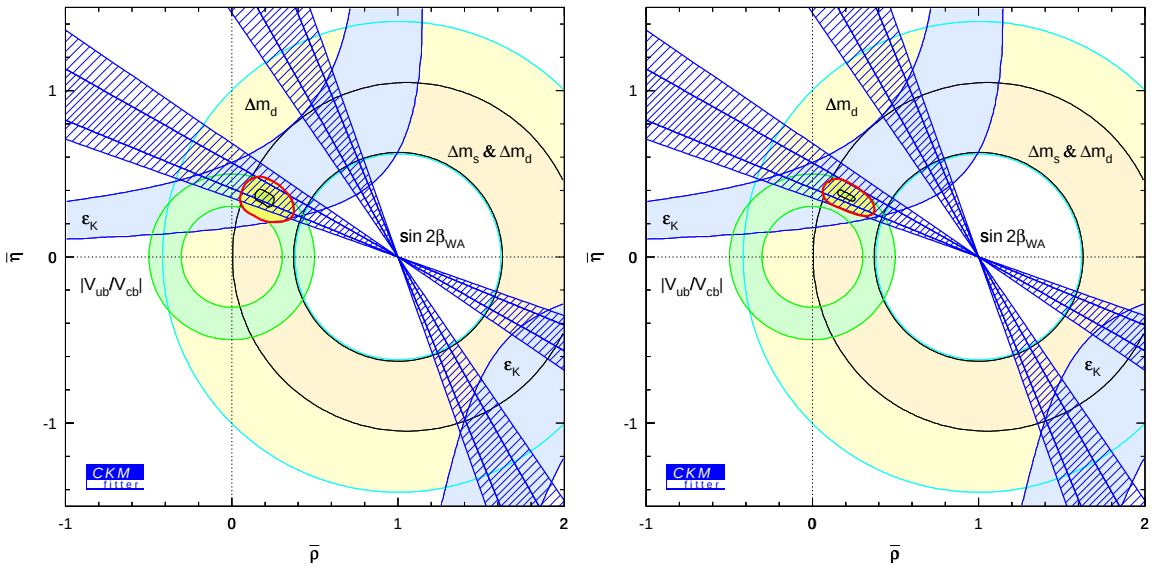

Figure 2: The standard CKM fit in the $\overline{\rho}-\overline{\eta}$ plane. Left: $> 5\%$ CL individual domains (the $\sin 2\beta$ WA is shown with its 1σ and 2σ bands) and the global fit without using the world average of $\sin 2\beta$. Right: including $\sin 2\beta$ in the combined fit. The inner zone indicates the importance of theoretical uncertainties, which is greatly reduced when including $\sin 2\beta$ in the fit.

confidence level as a function of Δm_s, to be used in the global fit [26].

The matrix elements of the effective four fermion couplings used to compute the box diagrams that mediate K and B mixing, are obtained from lattice QCD. Model-independent unquenched calculations are undertaken, but not yet precise enough for the needs in the global fit. In effect, with the exception of $\sin 2\beta$ and the inclusive determinations of $|V_{u(c)b}|$, the standard CKM fit is now in the hand of the Lattice community!

3.3 Fit results

The resulting confidence levels of the standard fit are displayed in the $\overline{\rho}-\overline{\eta}$ plane in Fig. 2. Also shown are the $> 5\%$ CL bands of the individual constraints, including the 4-fold ambiguity of the $\sin 2\beta$ measurement. *Its agreement with the indirect determination represents a triumph for the Standard Model and the KM paradigm [8]. It establishes the KM mechanism as the dominant source of CPV at the electroweak scale.* The inclusion of $\sin 2\beta$ (right hand plot in Fig. 2) into the standard fit significantly reduces the allowed region.

Parameter	95% CL region	Parameter	95% CL region
λ	0.2221 ± 0.0041	$\lvert V_{ud}\rvert$	0.97504 ± 0.00094
A	0.76 - 0.90	$\lvert V_{ub}\rvert$ $[10^{-3}]$	3.15 - 4.37
$\overline{\rho}$	0.08 - 0.35	$\lvert V_{cb}\rvert$ $[10^{-3}]$	36.9 - 43.6
$\overline{\eta}$	0.28 - 0.45	$\lvert V_{td}\rvert$ $[10^{-3}]$	6.3 - 9.1
J $[10^{-5}]$	2.2 - 3.5	$\lvert V_{ts}\rvert$ $[10^{-3}]$	36.4 - 43.0
$\sin 2\alpha$	-0.81 - 0.43	$\lvert V_{tb}\rvert$	0.99905 - 0.99932
$\sin 2\beta$	0.64 - 0.84	BR($K_{\rm L}^0 \to \pi^0\nu\overline{\nu}$) $[10^{-11}]$	1.6 - 4.2
α	77° - 117°	BR($K^+ \to \pi^+\nu\overline{\nu}$) $[10^{-11}]$	5.1 - 8.4
β	19.9° - 28.6°	BR($B^+ \to \tau^+\nu_\tau$) $[10^{-5}]$	7.2 - 22.1
$\gamma = \delta_{CP}$	40° - 78°	BR($B^+ \to \mu^+\nu_\mu$) $[10^{-7}]$	2.9 - 8.7

Table 3: Fit results for the unitary CKM parameters, the CKM matrix elements and branching ratios of some rare K and B meson decays *including the world average* $\sin 2\beta$ *in the fit*. Ranges are given for the quantities that are limited by systematic theoretical errors.

Table 3 lists 95% CL allowed domains of some relevant parameters, obtained from one-dimensional scans equivalent to those performed in the $\overline{\rho} - \overline{\eta}$ plane. The world average of $\sin 2\beta$ is always included in the fits. The procedure ensures the consistency of all numbers among each other and with the combined fit.

4 Beyond the Standard Fit

A precise measurement of rare K and B decays can greatly augment the available information on the CKM phase.

4.1 Rare K decays

The detection of a second $K^+ \to \pi^+\nu\overline{\nu}$ event has been announced early 2002 by the E787 Collaboration at Brookhaven [27], leading to a branching fraction of $(1.57^{+1.75}_{-0.82}) \times 10^{-10}$, which is compatible with the SM prediction [28] given in Table 3. A total of 5 to 10 SM events is expected to be detected at the successor experiment E949 at BNL [29], so that this channel becomes an interesting ingredient of the CKM fit. It should be noted that the translation of results on rare kaon decay into a measurement of $|V_{td}|$ and $\overline{\eta}$, respectively, requires a good knowledge of the matrix element $|V_{cb}|$ entering with its fourth power the SM predictions.

4.2 Rare B decays

The high luminosity B factories provide a detailed picture of rare, charmless B decays. We shall distinguish in the following two categories:

1. Semileptonic (FCNC) and radiative B decays, mediated by box and penguin diagrams.

2. Hadronic $b \to u(d,s)$ decays, mainly mediated by tree and penguin diagrams.

Since large virtual scales are involved, the first class of decays provides sensitive probes for new physics (SUSY, right-handed couplings, etc) via the measurements of rates and direct CPV. In addition, they can be used to determine the matrix elements $|V_{td}|$ and $|V_{ts}|$ as well as HQET parameters. Of particular interest is the measurement of the ratio $\Gamma(B \to \rho\gamma)/\Gamma(B \to K^*\gamma)$ which can be theoretically predicted to some accuracy [30, 31]. The present experimental upper limit is close to the the prediction obtained from the standard CKM fit so that a signal of the Cabibbo suppressed mode $B \to \rho\gamma$ is expected to be "just around the corner".

We will concentrate in the following on the second class of charmless B decays, allowing to measure CPV in the interference between decays with and without mixing and thus the determination of the UT angle α. The measurement of direct CP asymmetries and total rates provides information on the UT angle γ. Moreover, powerful tests of the factorization hypothesis can be performed.

Tge amplitudes of rare hadronic $B \to \pi\pi'$ decays into two pions are generally parameterized by:

$$A(B \to \pi\pi') = R_u e^{i\gamma} T + R_t e^{-i\beta} P \ , \tag{3}$$

$$A(\overline{B} \to \pi\pi') = R_u e^{-i\gamma} T + R_t e^{i\beta} P \ , \tag{4}$$

where T and P denote (complex) tree and penguin amplitudes, respectively. The CP transformation alters the sign of the weak phase only, since the strong interaction is assumed to be CP conserving. The parameters $R_u = |V_{ud}V_{ub}^*|$ and $R_t = |V_{td}V_{tb}^*|$ represent the sides of the UT. For decay modes into two pions the tree and penguin amplitudes are of the same order λ^3, while the tree is λ^4-suppressed and the penguin λ^2-enhanced in decays into one kaon and one pion. Interference of tree and penguin amplitudes of similar size can lead to significant rate differences between CP conjugated amplitudes, *i.e.*, may exhibit direct CPV in the experiment.

Bounds on γ

Pioneered by the work of Fleischer-Mannel [32], it has been shown by many authors that CP-averaged branching fractions of B decays into two pseudoscalers can be used

to infer constraints on the UT angle γ. The theoretical analysis deals among others with $SU(3)$ breaking, rescattering contributions (FSI) and electroweak penguins. One can define the following CP-averaged ratios [41]:

$$R \equiv \frac{\tau_{B^+}}{\tau_{B^0}} \frac{\Gamma(B^0 \to K^\pm \pi^\mp)}{\Gamma(B^\pm \to K^0 \pi^\pm)} = 1.07^{+0.15}_{-0.12} \quad (< 1\ ?)\ , \tag{5}$$

$$R_n \equiv \frac{1}{2} \frac{\Gamma(B^0 \to K^\pm \pi^\mp)}{\Gamma(B^0 \to K^0 \pi^0)} = 1.04^{+0.37}_{-0.22} \quad (\neq 1\ ?)\ , \tag{6}$$

$$R_c \equiv 2 \frac{\Gamma(B^\pm \to K^\pm \pi^0)}{\Gamma(B^\pm \to K^0 \pi^\pm)} = 1.24^{+0.24}_{-0.21} \quad (\neq 1\ ?)\ , \tag{7}$$

known as Fleischer-Mannel [32], Buras-Fleischer [33] and Neubert-Rosner (NR) [34] bounds, respectively. While Eq. (5) is required to be smaller than 1 to obtain non-trivial bounds on γ, the other two can lead to constraints once they significantly depart from 1 (see Ref. [35] for a further going analysis of these ratios). At present, only the addition of phenomenological or theoretical estimates on the size of the penguin amplitudes and/or the strong phases involved leads to significant information: Figure 3 shows on the left hand plot the NR bound (7) in the $\overline{\rho} - \overline{\eta}$ plane[4], when constraining the size of the tree-over-penguin ratio using the experimental values of $\Gamma(B^\pm \to \pi^\pm \pi^0)/\Gamma(B^\pm \to K^0 \pi^\pm)$ (tree-only over penguin-only ratio) together with a correction for $SU(3)$ breaking (and using naive factorization[5]). The constraints are weak compared to the current knowledge from the standard fit. Using in addition *QCD Factorization* (QCD FA) [36], which predicts small relative strong phases between tree and penguin amplitudes, does lead to a significant constraint (right hand plot in Fig. 3).

4.3 CPV in $B^0 \to \pi^+\pi^-$ decays

On the contrary to the golden mode $B^0 \to J/\psi K^0$, where penguin contributions with different weak phases are doubly-Cabibbo suppressed, the time-dependent CP-asymmetry analysis of $B^0 \to \pi^+\pi^-$ decays suffers from significant penguin pollution. As a consequence, both the sine and the cosine terms in the time evolution are unknown:

$$a_{CP}(t) = S_{\pi\pi} \sin(\Delta m_d \Delta t) - C_{\pi\pi} \cos(\Delta m_d \Delta t)\ , \tag{8}$$

with the time difference, Δt, between the CP and the tag side decay vertices, and the coefficients

$$S_{\pi\pi} = \frac{2\mathrm{Im}\lambda_{\pi\pi}}{1 + |\lambda_{\pi\pi}|^2} \quad \text{and} \quad C_{\pi\pi} = \frac{1 - |\lambda_{\pi\pi}|^2}{1 + |\lambda_{\pi\pi}|^2}\ . \tag{9}$$

[4]The R&D logo labels plots for which the discussion of theoretical uncertainties is not settled.

[5]Factorization is based on the concept of *color transparency*: since the energy release of the heavy-to-light transition is large, soft gluons do not interact with the small $q\overline{q}$ color dipole of the emitted meson.

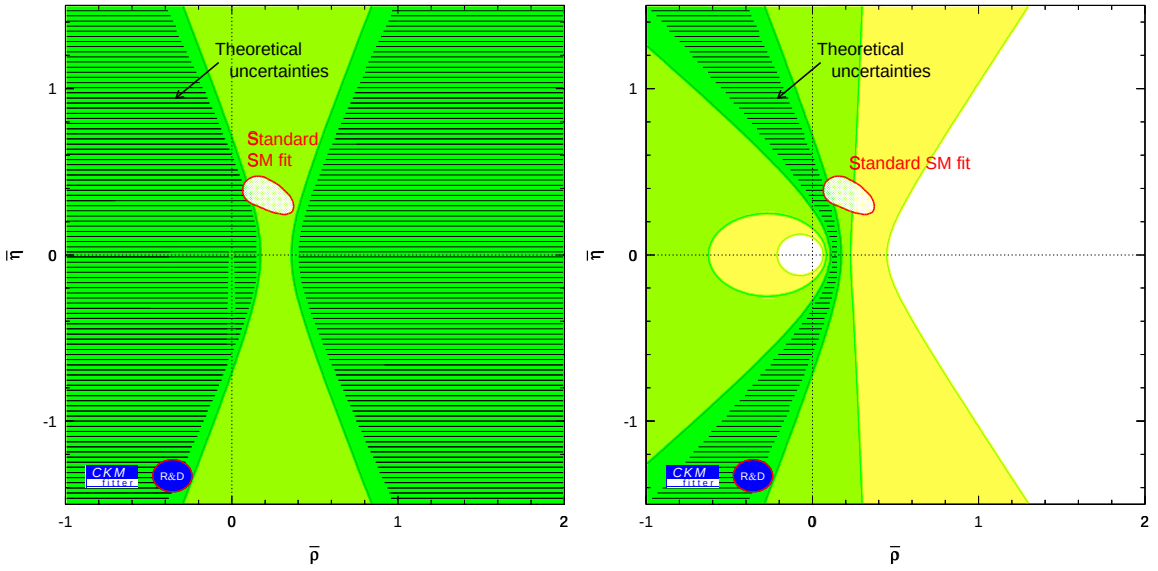

Figure 3: The Neubert-Rosner bound in the $\overline{\rho} - \overline{\eta}$ plane. Left: using a phenomenological constraint on the $|P/T|$ ratio and right: using in addition QCD FA, predicting small relative strong phases [36]. The shaded regions indicate the $\geq 5\%$, $\geq 32\%$ and $\geq 90\%$ CL domains. Also shown is the $> 5\%$ CL region of the standard CKM fit (including $\sin 2\beta$).

The CP parameter $\lambda_{\pi\pi}$ is given by the standard expression

$$\lambda_{\pi\pi} = e^{-2i\beta} \frac{A(\overline{B}^0 \to \pi^+\pi^-)}{A(B^0 \to \pi^+\pi^-)} = e^{2i\alpha} \frac{1 - (R_t/R_u)|P/T|e^{-i(\alpha-\delta)}}{1 - (R_t/R_u)|P/T|e^{+i(\alpha+\delta)}} \equiv |\lambda_{\pi\pi}| e^{2i\alpha_{\rm eff}} \ , \qquad (10)$$

where the phase $e^{-2i\beta}$ arises due to $B^0_d \overline{B}^0_d$ mixing and $R_{t(u)}$ are the sides of the UT (1), not to be confounded with the ratios (5-7). Note that $\pi^+\pi^-$ is a CP eigenstate with eigenvalue $+1$. In the presence of penguin contributions, the UT angle α is modified by the relative strong phase $\delta \equiv \arg(PT^*)$ between the penguin and the tree amplitudes. As a consequence, a measurement of the parameters $S_{\pi\pi}$ and $C_{\pi\pi}$ cannot be translated into $\sin 2\alpha$ without prior information on the strong phase difference δ and the ratio $|P/T|$. In principle, the Gronau-London isospin analysis [37] allows one to recover the missing pieces using the relations

$$\begin{aligned} A(B^+ \to \pi^+\pi^0) &= \frac{1}{\sqrt{2}} A(B^0 \to \pi^+\pi^-) + A(B^0 \to \pi^0\pi^0) \ , \qquad (11) \\ |A(B^+ \to \pi^+\pi^0)| &= |A(B^- \to \pi^-\pi^0)| \ , \end{aligned}$$

where electroweak penguins have been neglected. However, the unknown tagged rates for $B^0(\overline{B}^0) \to \pi^0\pi^0$, precludes from a complete application and only permits to

Observable	Value	Source
$\mathcal{B}(B^0 \to \pi^+\pi^-)$	$(5.2 \pm 0.6) \times 10^{-6}$	WA [41]
$\mathcal{B}(B^\pm \to \pi^\pm\pi^0)$	$(4.9 \pm 1.1) \times 10^{-6}$	WA [41]
$\mathcal{B}(B^0 \to \pi^0\pi^0)$	$< 3.4 \times 10^{-6}$ (90% CL)	*BABAR* [41]
$S_{\pi\pi}$	-0.01 ± 0.38	*BABAR* [42]
	$-1.21^{+0.41}_{-0.30}$	Belle [43]
$C_{\pi\pi}$	-0.02 ± 0.30	*BABAR* [42]
	$-0.94^{+0.32}_{-0.27}$	Belle [43] [sign convention reversed]

Table 4: Experimental results on $B \to \pi\pi$ decays used for the Gronau-London isospin analysis [37]. Statistical and systematic errors have been added in quadrature.

derive bounds on the difference $|\alpha - \alpha_{\text{eff}}|$. This has been first exploited by Grossman-Quinn [38] and Charles [39] and was further improved by Gronau-London-Sinha-Sinha [40]. While the evaluation of the above bounds gives an interesting insight into the structure of the isospin relations, it is by no means a necessary exercise. Indeed, since no additional input is used it merely represents a reformulation of Eqs. (11). Numerical analysis tools like *CKMfitter* automatically exploit the information from the bounds once they dispose of the input observables and the isospin relations. Moreover, it guarantees the optimal use of the totality of the constraints provided.

It is instructive to follow a hierarchy of approaches, using more and more theoretical input to constrain the CKM phase:

(A) using as input $C_{\pi\pi}$ and $S_{\pi\pi}$ as well the branching fractions $B \to \pi\pi$ ($\pi \in \{\pi^+, \pi^0\}$) and strong isospin.

(B) using (A) and $B^0 \to K^+\pi^-$ together with $SU(3)$ (neglecting OZI-suppressed penguin annihilation topologies [39]).

(C) using (B) and the determination of $|P/T|$ by means of the rates of the decays $B^+ \to \pi^+\pi^0$ and $B^+ \to K^0\pi^+$ and $SU(3)$ and naive factorization, but leaving the relative strong phase unconstrained.

(D) using (B) and the prediction of the complex P/T ratio (absolute value and phase) by means of QCD Factorization.

We will only show results for the items (A) and (D) in these proceedings. The experimental measurements used are given in Table 4. We consider the *CP* asymmetry results obtained by *BABAR* and Belle to be incompatible at present and thus treat

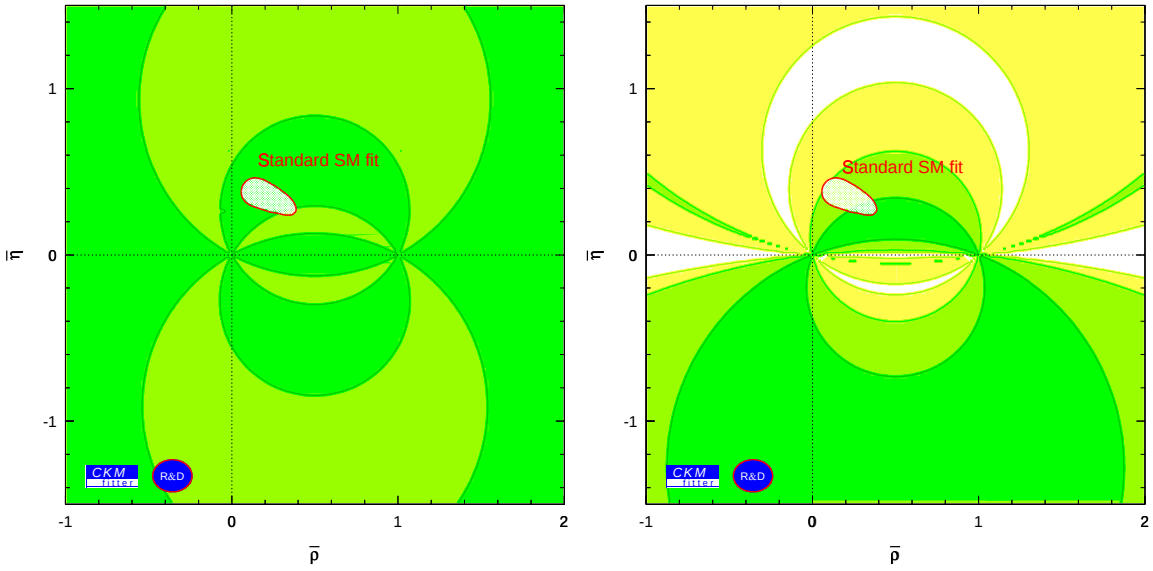

Figure 4: Results on $\pi\pi$ in the $\overline{\rho}-\overline{\eta}$ plane using the Gronau-London isospin analysis. Left: using $S_{\pi\pi}$ and $C_{\pi\pi}$ from *BABAR*, right: Belle. The shaded regions indicate the $\geq 5\%$, $\geq 32\%$ and $\geq 90\%$ CL domains. Also shown is the $> 5\%$ CL region of the standard CKM fit (including $\sin 2\beta$).

them independently. Figure 4 shows the constraints obtained by the isospin analysis applying the experimental limit on the rate of $B^0 \to \pi^0\pi^0$ (*BABAR*) and using time-dependent *CP* asymmetry results from *BABAR* (left) and Belle (right). Both experiments agree with the standard fit within the large uncertainties from the weak bound on the penguin contribution. To turn this approach into a competitive method, either the branching fraction of $B^0 \to \pi^0\pi^0$ has to be significantly lower than 10^{-6}, or very large luminosity is required to precisely measure their tagged rates.

As a subsequent, more promising but also less robust approach, we shall apply the full QCD FA [36] prediction of the complex P/T ratio to constrain α via Eq. (9). The resulting constraints in the $\overline{\rho}-\overline{\eta}$ plane are plotted in Fig. 5. We find that the *BABAR* result is well within the expected range, whereas—not surprisingly—the Belle numbers prefer a larger phase and $|P/T|$ ratio. The agreement of the latter with the standard fit is on the 10% level. The upper right hand plot shows the *BABAR* results on $S_{\pi\pi}$ and $C_{\pi\pi}$ together with the world average of $\sin 2\beta$. It visualizes the impressive constraint already obtained from the time-dependent analyses of the B factories alone.

One may reverse Eq. (9) and inject the result of the standard fit on α in order to probe the relative strong phase and the $|P/T|$ ratio in a model-independent matter.

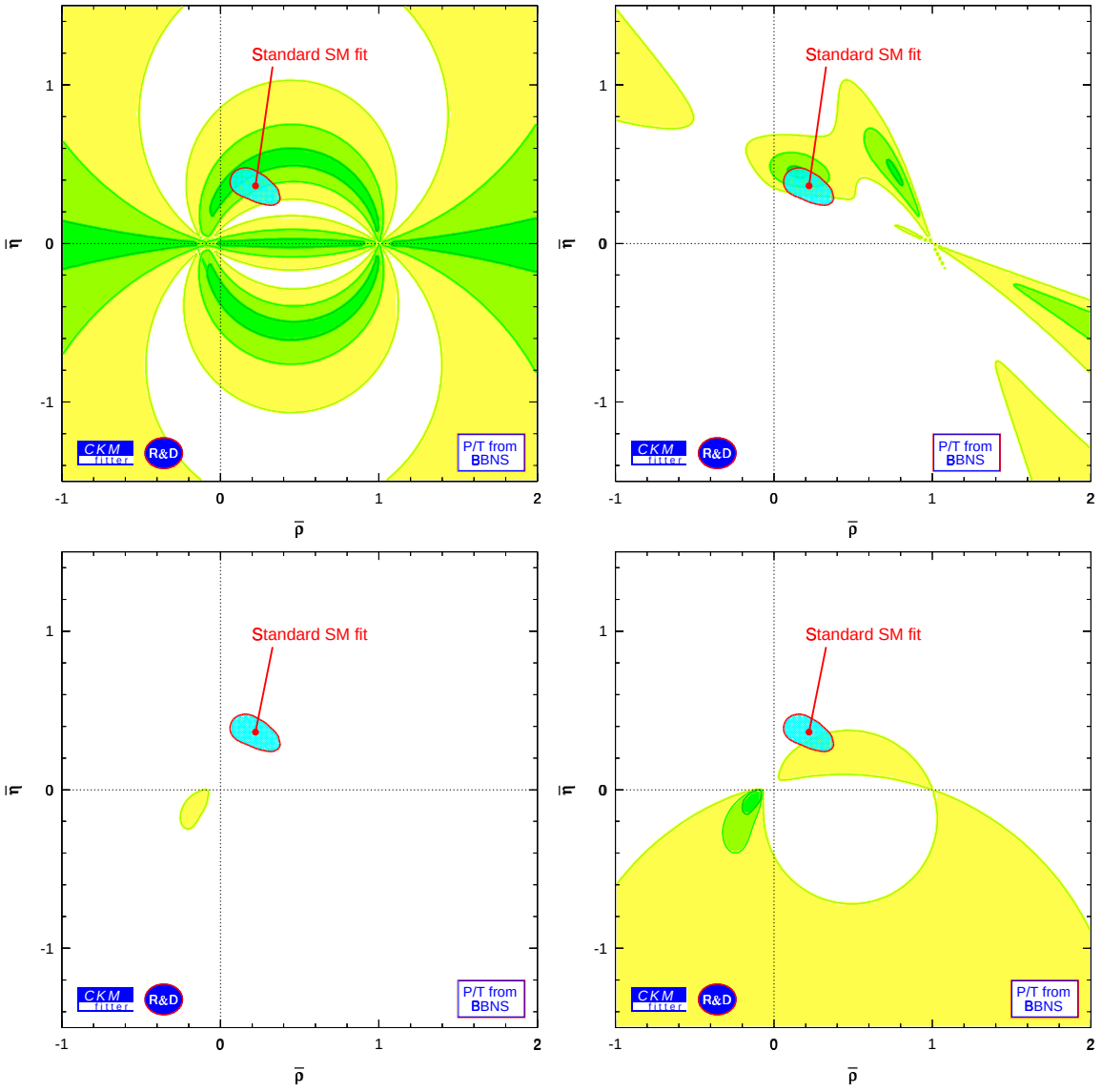

Figure 5: Upper plot: *BABAR* results on $\pi^+\pi^-$ in the $\overline{\rho} - \overline{\eta}$ plane using the QCD FA [36] prediction of the penguin contribution and strong phase difference. The upper right hand plot shows the combined results for the *CP* asymmetry measurements using charmonium modes and $\pi^+\pi^-$ (*BABAR*). Lower plots: the corresponding results from Belle. The right hand plot zooms the CLs between 0 and 10%. Also shown in all plots is the $> 5\%$ CL region of the standard CKM fit (including $\sin 2\beta$).

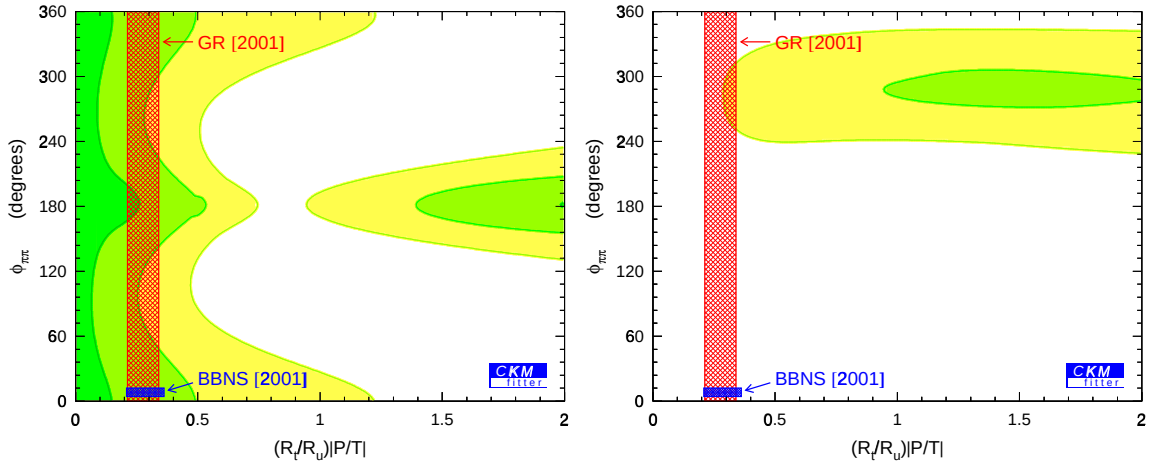

Figure 6: The $S_{\pi\pi}$ and $C_{\pi\pi}$ measurements of *BABAR* (left) and Belle (right) are used to determine the relative strong phase (ordinate) and the penguin-to-tree ratio (abscissa). The value of the UT angle α of the standard CKM fit is injected with its uncertainties. The allowed regions are compared to theoretical predictions [36, 44].

The resulting confidence levels are given in Fig. 6. As expected, the *BABAR* result (left) agrees with QCD FA while Belle prefers larger phases. However, it is important to note that these observations are tendencies only, not yet supported by statistically significant results.

5 Conclusions

The successful operation of the B factories at SLAC and KEK has provided a flood of new results that can be used to obtain information on the CP-violating phase of the CKM matrix. The extraordinary agreement of the world average of $\sin 2\beta$ with the indirect determination represents a triumph for the Standard Model and the KM paradigm. It establishes the KM mechanism as the dominant source of CPV at the electroweak scale. While the inclusion of $\sin 2\beta$ into the global CKM fit is a grateful task, exploiting rare B decays requires some theoretical digestion in order to lead to meaningful constraints at present.

We now constrain the center of the $\overline{\rho}-\overline{\eta}$ plane to quite some accuracy, albeit it is still too large to seriously challenge the Standard Model at the percent level. Obviously, a better understanding of long distance QCD opens the shrine to a full exploitation of the huge data samples currently produced at KEK-B and PEP-II, and the tremendous data quantities that will be produced at the TEVATRON and the LHC. Much hope is sent towards the Lattice community in this respect. Will we be able to discover

signs of new physics before the advent of the LHC?

This conference was a true pleasure: for it's scientific program and the attendance as well as for the smooth organization. My sincere thanks are dedicated to the local organization committee. I am indebted to the fruitful and pleasant collaboration with Heiko Lacker, Sandrine Laplace, Franccois Le Diberder, José Ocariz and Muriel Pivk.

References

[1] *BABAR* Collaboration (B. Aubert *et. al.*), Phys. Rev. Lett. **86**, 2515 (2001)

[2] Belle Collaboration (A. Abashian *et. al.*)), Phys. Rev. Lett. **86**, 2509 (2001)

[3] I.I. Bigi, Talk given at Meson 2002, Cracow, Poland, 24-28 May 2002, UND-HEP-02-BIG-05, TTP-02-10, [hep-ph/0206261]

[4] F. Parodi, P. Roudeau and A. Stocchi, Nuovo Cim. **A112** 833 (1999)

[5] M. Hazumi (Belle) and S. Rahatlou (*BABAR*), *these proceedings*

[6] For a description of *CKMfitter* and the source code as well as links to the newest plots and presentations, consult the web site:
http://ckmfitter.in2p3.fr/

[7] A. Höcker, H. Lacker, S. Laplace and F. Le Diberder, Eur. Phys. J. **C21**, 225 (2001), [hep-ph/0104062]

[8] M. Kobayashi and T. Maskawa, *Prog. Theor. Phys.* **49** (1973) 652; N. Cabibbo, *Phys. Rev. Lett.* **10** (1963) 351

[9] Several groups have pioneered global CKM fits in the past. For the attempt of an exhaustive list, please see Ref. [8] of [7]

[10] L. Wolfenstein, Phys. Rev. Lett. **51**, 1945 (1983)

[11] A.J. Buras, M.E. Lautenbacher and G. Ostermaier, Phys. Rev. **D50**, 3433 (1994)

[12] C. Jarlskog, Phys. Rev. Lett. **55**, 1039 (1985)

[13] S. Laplace, Z. Ligeti, Y. Nir and G. Perez, Phys. Rev. **D65**, 094040 (2002)

[14] H. Abele et al., Phys. Rev. Lett. **88**, 211801 (2002)

[15] CLEO Collaboration (A. Bornheim *et. al.*), Phys. Rev. Lett. **88**, 231803 (2002); (D. Cronin-Hennessy *et. al.*), Phys. Rev. Lett. **87**, 251808 (2001);

[16] LEP $|V_{ub}|$ Working Group (2001),
http://battagl.home.cern.ch/battagl/vub/vub.html

[17] CLEO Collaboration (B.H. Behrens *et. al.*), Phys. Rev. **D61**, 052001 (2000)

[18] Belle Collaboration (K. Abe et al.), Phys. Rev. Lett. **88**, 231803 (2002

[19] CLEO Collaboration (R.A. Briere *et. al.*), CLNS-01-1773, CLEO-01-26 (2002), [hep-ex/0203032]

[20] CLEO Collaboration Phys Rev lett **87**, 251808 (2001)

[21] LEP $|V_{cb}|$ Working Group (Winter 2002),
http://lepvcb.web.cern.ch/LEPVCB/

[22] LEP B Oscillation Working Group (Moriond 2002),
http://lepbosc.web.cern.ch/LEPBOSC/

[23] A. Kronfeld, *these proceedings*

[24] M. Luke, *these proceedings*

[25] A.S. Kronfeld, S.M. Ryan, FERMILAB-PUB-02-109-T (2002), [hep-ph/0206058]

[26] F. Le Diberder, contribution to WG II of the CERN CKM Workshop (2002),
http://ckm-workshop.web.cern.ch/ckm-workshop/

[27] E787 Collaboration (S. Adler *et. al.*), Phys. Rev. Lett. **88**, 041803 (2002)

[28] G. Buchalla and A. Buras, Nucl. Phys. **B398**, 285 (1993); Nucl. Phys. **B400**, 225 (1993); Nucl. Phys. **B548**, 309 (1999)

[29] The E949 web site:
http://www.phy.bnl.gov/e949/

[30] A. Ali, A.Y. Parkhomenko, Eur. Phys. J. **C23**, 89 (2002)

[31] S.W. Bosch, G. Buchalla, Nucl. Phys. **B621**, 459, 2002

[32] R. Fleischer and T. Mannel, Phys. Rev. **D57**, 2752 (1998)

[33] A. Buras and R. Fleischer, Eur. Phys. J. **C11**, 93 (1998)

[34] M. Neubert and J.L. Rosner, Phys. Lett. **B441**, 403 (1998)

[35] M. Bargiotti *et. al.*, Eur. Phys. J. **C24**, 361 (2002)

[36] M. Beneke, G. Buchalla, M. Neubert and C.T. Sachrajda, Nucl. Phys. **B606**, 24 (2001)

[37] M. Gronau and D. London, Phys. Rev. Lett. **65**, 3381 (1990)

[38] Y. Grossman and H.R. Quinn, Phys. Rev. **D58**, 017504 (1998)

[39] J. Charles, Phys. Rev. **D59**, 054007 (1999)

[40] M. Gronau, D. London, N. Sinha, R. Sinha, TECHNION-PH-2001-27, UdeM-GPP-TH-01-89, IMSc-2001/05/27 (2001), [hep-ph/0105308]

[41] R. Bartoldus, *these proceedings*

[42] P. Dauncey (*BABAR*), *these proceedings*

[43] E. Won (Belle), *these proceedings*

[44] M. Gronau and J.L. Rosner, Phys. Rev. **D65**, 013004 (2002)